ISBN: 978-3-95450-230-1 ISSN: 2673-5350 doi:10.18429/JACoW-IBIC2021-WEPP06

OBSERVATION AND ANALYSIS OF ISLAND PHENOMENON IN THE STORAGE RING LIGHT SOURCE*

Yunkun Zhao, Sanshuang Jin, Jigang Wang†, Baogen Sun‡, Fangfang Wu, Tianyu Zhou, Ping Lu, Leilei Tang,
National Synchrotron Radiation Laboratory (NSRL),
University of Science and Technology of China (USTC), Hefei, China

Abstract

In the previous experimental investigations and measurements using the radio-frequency (RF) phase modulation method to study the longitudinal beam characteristics of the Hefei Light Source-II (HLS-II), we found that the longitudinal bunch distributions under different modulation frequencies and amplitudes have great difference. In order to further explore island phenomenon and better understand beam motion associated with external RF phase modulation, the streak camera is exploited to effectively observe the longitudinal bunch profile and distribution in single-bunch filling mode. In addition, the dependence between island size, bunch dilution effect and modulation frequency are also discussed in detail. This is meaningful for researching the impact of RF noise on longitudinal beam dynamics, beam manipulation, and machine maintenance and debugging.

INTRODUCTION

In accelerators, the investigation of the nonlinear longitudinal beam dynamics [1,2] is of great physical significance and engineering value. This is particularly important for studying and exploring the mechanism of beam instability, analysis of beam evolution, observation of longitudinal bunch characteristics, and beam manipulation. In the actual operation of accelerators and synchrotron radiation light sources, particle motion is generally disturbed by RF noise, wakefields, power supply ripple, vibration, etc. There is no doubt that these disturbances will cause changes in beam motion and machine performance due to RF phase and voltage modulations. A part of the theoretical analysis and experimental measurements have been demonstrated that this RF modulation has significant advantages as that of suppressing the coupled bunch instability, improving the beam lifetime, and performing beam manipulation in phase space. Therefore, the RF phase modulation (RFPM) technique was preferred introduced into the HLS-II storage ring to deeply research longitudinal beam characteristics and effectively improve beam lifetime in recent research work [3,4]. However, it is a pity that the exploration of the nonlinear longitudinal beam dynamics is not comprehensive and ambiguous in the presence of the RFPM error noise. Moreover, some clerical errors need to be corrected in reference [3]. As a consequence, the motivation of this article is to further investigate the nonlinear beam dynamics in HLS-II based on the RFPM approach. The main research contents include the observation of resonance island phenomenon, characterization of island size, and study of transient beam response.

THEORETICAL MODELLING AND ANALYSIS

In the synchrotron radiation light sources, when charged particles are suffered from RFPM, the effective parametric resonance Hamiltonian equation can be expressed as [1,2]

$$\begin{aligned} H(\delta,\phi) = {} & \frac{\omega_s\delta^2}{2} + \omega_s \tan\phi_{s0}\left[\sin\phi\cos\left(a_m\sin\omega_m t\right)\right. \\ & \left.+\cos\phi\sin\left(a_m\sin\omega_m t\right)\right] \\ & -\omega_s\cos\phi\cos\left(a_m\sin\omega_m t\right) \\ & +\omega_s\sin\phi\sin\left(a_m\sin\omega_m t\right) - \omega_s\sin\phi\tan\phi_{s0} \end{aligned} \tag{1}$$

In Eq. (1), ω_s denotes the synchronous oscillation angular frequency with $\omega_s = 2\pi f_s$, in which f_s denotes the synchrotron oscillation frequency. It is noted that ϕ_{s0} is determined by the synchrotron phase ϕ_s, namely equivalent to $\phi_{s0} = \pi - \phi_s$. a_m indicates the modulation amplitude, and ω_m indicates the angular frequency of RFPM that is satisfied with $\omega_m = 2\pi f_m$ where f_m is the modulation frequency. δ and ϕ are the energy deviation and the phase, respectively.

In the case that the RFPM frequency is close to the synchrotron frequency, for which the violent first-order parametric resonance can be produced at this time. After through coordinate transformation (J,ψ) and a series of simplifications and ignoring non-parametric resonance terms, the time-averaged Hamiltonian can be described by [5]

$$\langle H\rangle_t = \left(\omega_s - \omega_m\right)J - \frac{\omega_s J^2}{16} - \frac{\omega_s a_m}{2}(2J)^{\frac{1}{2}}\cos\psi \tag{2}$$

By introducing the feature function g, the solution of the above Eq. (2) can be written as

$$\begin{cases} g_1(x) = -\frac{8}{\sqrt{3}}\sqrt{x}\cos\frac{\xi}{3}, & (\mathrm{SFP},\psi=\pi) \\ g_2(x) = \frac{8}{\sqrt{3}}\sqrt{x}\cos\left(\frac{\pi}{3}+\frac{\xi}{3}\right), & (\mathrm{SFP},\psi=0) \\ g_3(x) = \frac{8}{\sqrt{3}}\sqrt{x}\cos\left(\frac{\pi}{3}-\frac{\xi}{3}\right), & (\mathrm{UFP},\psi=0) \end{cases} \tag{3}$$

* Work supported by the National Natural Science Foundation of China under Grant 12075236, Grant 12005223, Grant 51627901, and Grant 11705203, the Anhui Provincial Natural Science Foundation under Grant 1808085QA24, and the Fundamental Research Funds for the Central Universities under Grant WK2310000080.
† wangjg@ustc.edu.cn
‡ bgsun@ustc.edu.cn

ISBN: 978-3-95450-230-1 ISSN: 2673-5350 doi:10.18429/JACoW-IBIC2021-WEPP06

where $x = 1 - \omega_m/\omega_s$, $x_{\rm bif} = 1 - \omega_{\rm bif}/\omega_s$, $\xi = \arctan(\sqrt{\left(\frac{x}{x_{\rm bif}}\right)^3 - 1})$, and the bifurcation angular frequency is $\omega_{\rm bif} = \omega_s \left[1 - \frac{3}{16}(4a_m)^{\frac{2}{3}}\right]$. Here, it is especially emphasized that g_1 and g_2 stand for the outer and the inner stable fixed points (SFPs), whereas g_3 for the unstable fixed point (UFP). These fixed points act as the attractors whose role are to draw and capture the charged particles to move in the longitudinal phase space, for which leads to the formation of the resonant islands or beamlets. Of course, the particle distribution and bunch density can be effectively manipulated by means of RFPM. According to the aforementioned theoretical model Eqs. (2)– (3), numerical simulations are carried out based on the core parameters of HLS-II [3], as shown in Fig. 1.

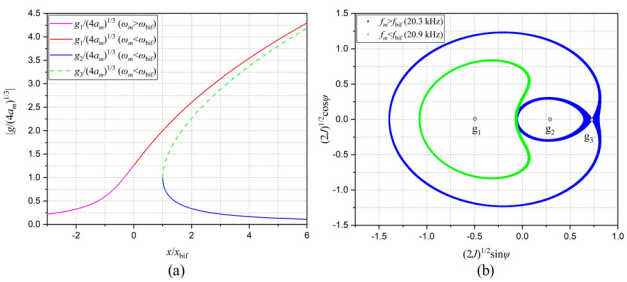

Figure 1: The phase amplitudes of fixed points and Hamiltonian tori in phase space (the simulated parameters are: $a_m = 0.02$ rad, $f_s = 21.3$ kHz, and $f_{\rm bif} = 20.6$ kHz).

In Fig. 1, it can be seen that the phase amplitude of the fixed point and the Hamiltonian torus are significantly different with the variation of the modulation frequency. As the modulation frequency is smaller than the bifurcation frequency, two SFPs and one UFP appear. This means that there are at least two resonant islands in the beam manipulation and bunch intensity dilution process. However, when the modulation frequency is larger than the bifurcation frequency, there is only one real solution to Eq. (3), yields

$$g_1(x) = -(4a_m)^{1/3}\left[\left(\sqrt{1-\left(\frac{x}{x_{\rm bif}}\right)^3}+1\right)^{1/3} - \left(\sqrt{1-\left(\frac{x}{x_{\rm bif}}\right)^3}-1\right)^{1/3}\right] \quad (4)$$

From Eq. (4), it is indicated that there is an island generated in the presence of RFPM. It is necessary to especially note that the resonance islands can be generated or annihilated owning to the transient and unstable beam response for the case that the modulation frequency is close to bifurcation frequency. For simplicity and convenience, it is straightforward to take advantage of the mixture of multi-Gaussian equation for analyzing the size of the resonant islands and beam dilution rate in the practical experimental measurements.

$$I(\tau) = I_0 + \sum_{i=1}^{n} I_i \exp\left[-\frac{(\tau - \overline{\tau}_i)^2}{2\sigma_i^2}\right] \quad (5)$$

Here, I_0 is the initial beam intensity, I_i is the peak value of the distribution, i is the number of islands, and σ_i is the width of i-th island. In this way, the island phenomenon caused by RFPM can be effectively quantitatively described and analyzed. According to Eq. (5), the simulated longitudinal bunch profiles of bi-Gaussian and multi-Gaussian cases are distinctly shown in Fig. 2.

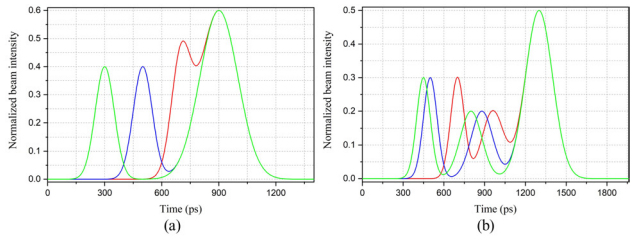

Figure 2: Longitudinal bunch profiles of bi-Gaussian and multi-Gaussian models.

EXPERIMENTAL SETUP AND RESULTS

In terms of the above-mentioned theoretical analysis, the RFPM is applied onto the RF system to observe the longitudinal bunch distribution and explore the island phenomenon. The experimental measurement system is clearly depicted in Fig. 3.

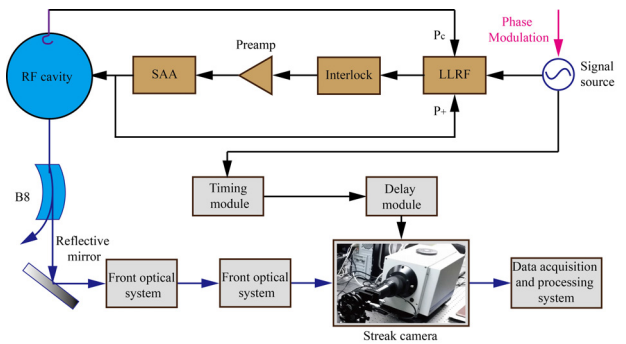

Figure 3: Diagram of the experimental measurement system for RFPM (the beam current is in the range of 11–13 mA with top-off mode).

As shown in Fig. 3, the RFPM experimental measurement system mainly consists of a RF cavity system and a streak camera measurement system. In the RF system, the 204 MHz RF signal output by the signal source is transmitted into the interlock module after the digital low-level RF (LLRF) system. And then it is fed into the solid-state amplifier (SSA) system after passing through the pre-amplifier, and finally 9.3 kW of power output from SSA propagated onto the RF cavity. Furthermore, the power signal coupled from the SSA and RF cavity is sent to the LLRF system as a feedback signal, of which is further delivered into the Free Programmable

ISBN: 978-3-95450-230-1 ISSN: 2673-5350 doi:10.18429/JACoW-IBIC2021-WEPP06

Gate Array (FPGA) board for control calculation after down-conversion and analog-to-digital conversion in the digital LLRF system. Notice that the interlock module is connected with three protection signals that is used to ensure the safety of personnel and machine.

It should be pointed out that the RFPM is applied to the signal source, and then affects the bunch motion in HLS-II. At the same time, the longitudinal bunch distribution and island effect subjected to RFPM are measured and observed by the streak camera measurement system installed downstream at the diagnostic beamline B8. Further, we obtained the longitudinal bunch intensity images and distributions without and with RFPM as shown in Figs. 4 and 5, respectively.

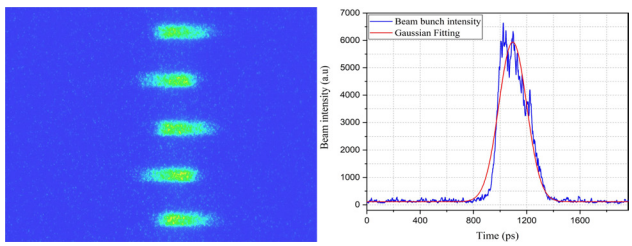

Figure 4: Longitudinal bunch intensity image and profile in the absence of RFPM.

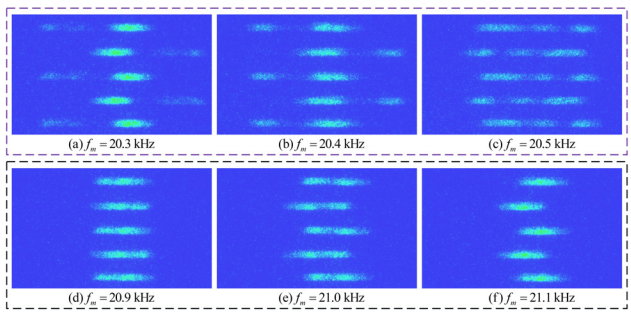

Figure 5: Longitudinal bunch intensity image versus RFPM frequency.

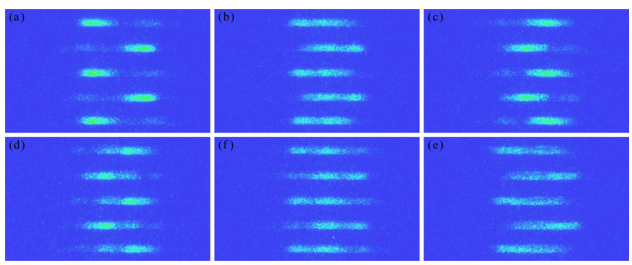

Figure 6: Observations of the longitudinal bunch structures in transient response under the modulation frequency of 20.6 kHz.

Figure 4 shows the bunch intensity and distribution without RFPM, and the blue and red lines are the longitudinal bunch profile and corresponding fitting curve, respectively. Through in-depth data-analysis, the root-mean-square (rms) bunch length can be acquired as 104.3 ps. In Fig. 5, the upper trace reveals the longitudinal bunch intensity images when the RFPM frequency is 20.3, 20.4, and 20.5 kHz, respectively, near the bifurcation frequency of 20.6 kHz. Nevertheless, the lower trace reveals the longitudinal bunch intensity images as that of the modulation frequency of 20.9, 21.0, and 21.1 kHz, individually, exceeding the bifurcation frequency. It is observed from Fig. 5 that the introduced RFPM can effectively manipulate the beam intensity and elongate bunch length. Additionally, it can be clearly seen that the RF phase error noise can produce the dramatic island phenomena. This main reason is that when the nonlinear parametric resonance will occur when the modulation frequency approaches to the synchrotron frequency, of which results in the dilution of bunch density, and simultaneously to stretch the bunch length and form the resonant islands. Here, it is emphasized that this island effect is the transient response of beam, with which the island can be generated or annihilated as the case that the modulation frequency is close to the bifurcation frequency, as shown in Fig. 6. As a result, the island phenomenon can be utilized for roughly analysing and evaluating the impact of the existed RF noise on beam characteristics in the storage ring light source. Indeed, this has certain reference and application value for machine study and beam evolution exploration in the actual accelerator operation.

In order to further analyze and discuss the island phenomenon, the mixed multi-Gaussian model is exploited to quantize the width of island and the beam dilution effect at various RFPM frequencies, as shown in Figs. 7 and 8, respectively.

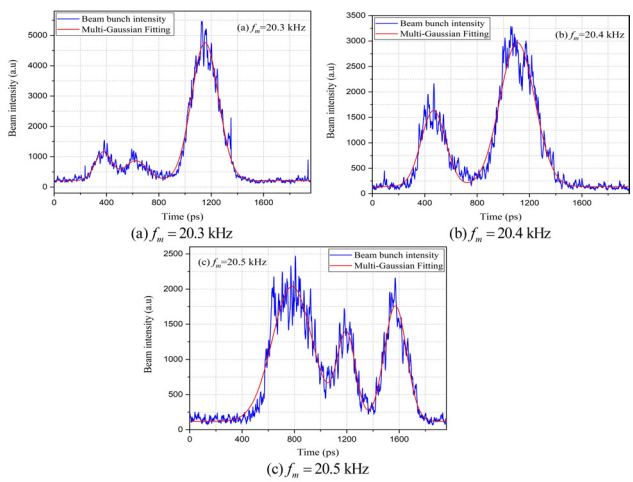

Figure 7: Longitudinal bunch distributions and data-analysis below the bifurcation frequency.

Figure 7 expresses the longitudinal bunch distributions and according fitting curves corresponding to the RFPM frequency of 20.3, 20.4, and 20.5 kHz, respectively, below the bifurcation frequency. Nevertheless Fig. 8 depicts the longitudinal bunch distributions and according fitting curves in the case of the RFPM frequency exceeding the bifurcation frequency of 20.9, 21.0, and 21.1 kHz, respectively. From detailed data analysis, the rms widths of the formed reso-

ISBN: 978-3-95450-230-1 ISSN: 2673-5350 doi:10.18429/JACoW-IBIC2021-WEPP06

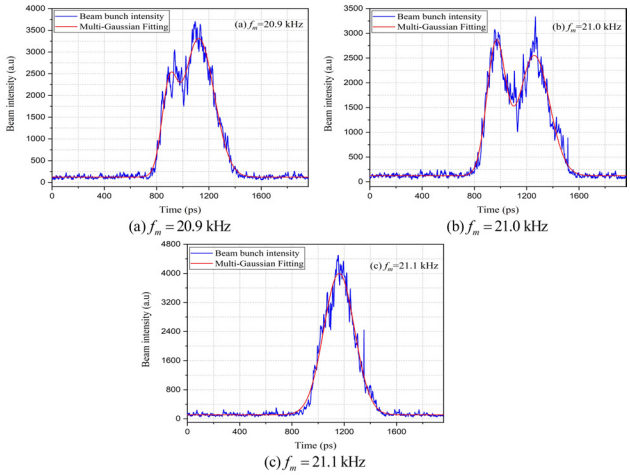

Figure 8: Longitudinal bunch distributions and data-analysis above the bifurcation frequency.

nance islands are obtained to be 62.5 ps/45.1 ps/72.9 ps, 66.9 ps/94.6 ps, and 108.3 ps/50.0 ps/60.7 ps, which correspond to the RFPM frequencies are 20.3, 20.4, and 20.5 kHz, respectively. And the island widths are 41.0 ps/83.4 ps, 50.2 ps/82.9 ps, and 117.5 ps when the RFPM frequencies are finely adjusted to be 20.9, 21.0, and 21.1 kHz, respectively. It is apparent that the beam dilution effect becomes more significant as the width of the island increases as a result of RFPM.

CONCLUSION

In this paper, the RFPM method is used for researching the longitudinal bunch distribution and nonlinear island phenomenon on HLS-II. It has shown that the generation of the resonant island and the beam dilution effect are dependent on the RFPM frequencies and amplitudes. In addition, the mixed multi-Gaussian theoretical model is developed to analyze the size of the resonance island and effectiveness of beam manipulation. This is useful and meaningful for the analysis of the influence of RF noise, investigation of the longitudinal beam dynamics, exploration of the nonlinear island phenomena, maintenance and debugging of machine.

ACKNOWLEDGEMENTS

This work was supported in part by the National Natural Science Foundation of China under Grant 12075236, Grant 12005223, Grant 51627901, and Grant 11705203, the Anhui Provincial Natural Science Foundation under Grant 1808085QA24, and the Fundamental Research Funds for the Central Universities under Grant WK2310000080.

REFERENCES

[1] H. Huang *et al.*, "Experimental determination of the Hamiltonian for synchrotron motion with rf phase modulation", *Phys. Rev. E*, vol. 48, no. 6, pp. 4678–4688, 1993. doi:10.1103/PhysRevE.48.4678

[2] N. P. Abreu *et al.*, "Longitudinal dynamics with rf phase modulation in the Brazilian electron storage ring", *Phys. Rev. ST Accel. Beams*, vol. 9, no. 12, p. 124401, 2006. doi:10.1103/PhysRevSTAB.9.124401

[3] Y. Zhao *et al.*, "Experimental research on HLS-II performance by means of the RF phase modulation technique", *IEEE T. Nucl. Sci.*, vol. 68, no. 2, pp. 92–100, 2021. doi:10.1109/TNS.2020.3040266

[4] Y. Zhao *et al.*, "Effect of phase modulation on the transverse beam size and emittance of the HLS-II ring", in *Proc. 9th Int. Beam Instrumentation Conf. (IBIC'20)*, Santos, Brazil, Sep. 2020, paper WEPP26, pp. 158–161. doi:10.18429/JACoW-IBIC2020-WEPP26

[5] S. Y. Lee, "Synchrotron motion", in *Accelerator Physics*, Singapore: World Scientific, 2018, pp. 260–264.